Supporting Information

Highest-T_c Single-Component Homochiral Organic Ferroelectrics

Peng-Fei Li, † *Yong Ai,* † *Yu-Ling Zeng, Jun-Chao Liu, Zhe-Kun Xu and Zhong-Xia Wang* *

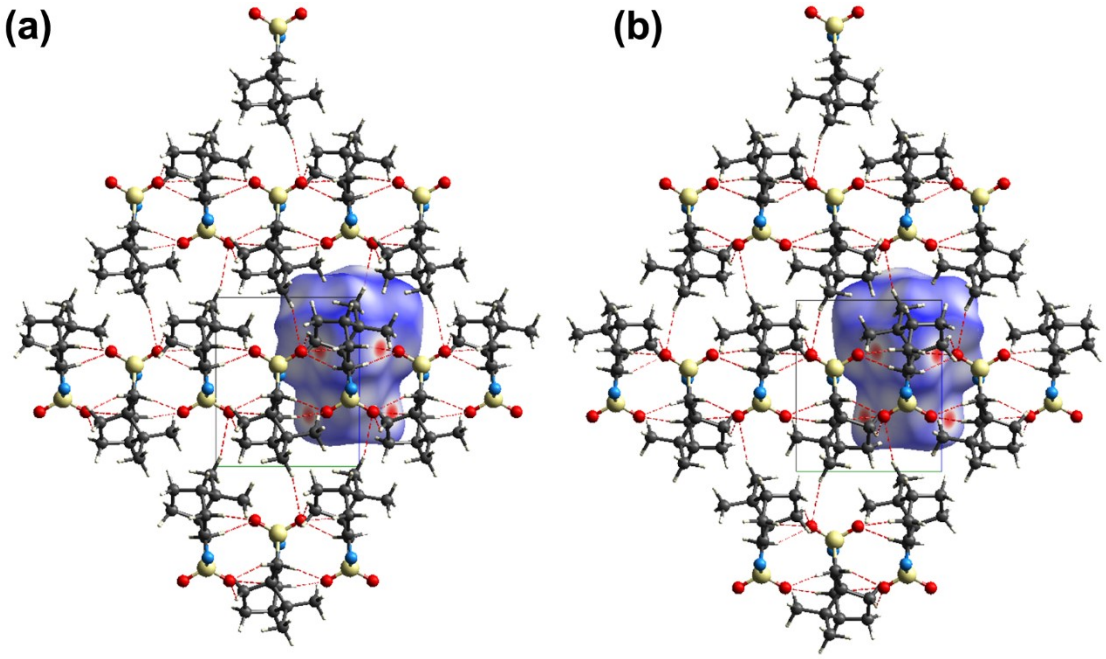

Fig. S1 Comparison of the Hirshfeld dnorm surfaces of *R*-CSAI (a) and *S*-CSAI (b), and their weak van der Waals forces forming the framework.

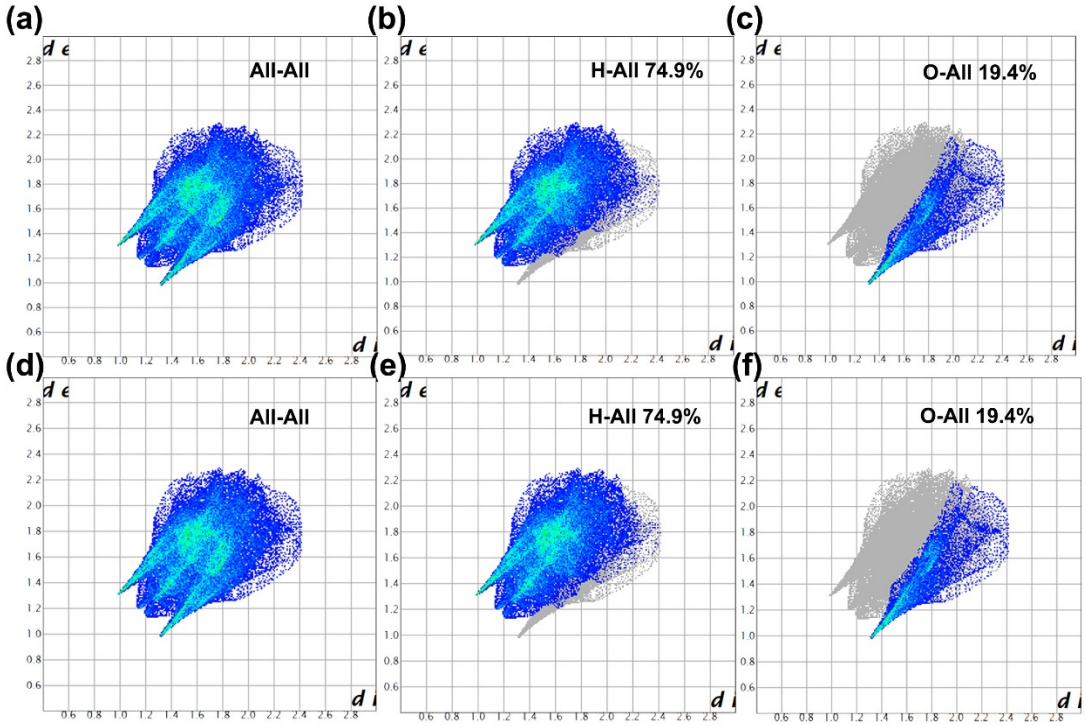

Fig. S2 2D fingerprint plots for *R*-CSAI (a) and *S*-CSAI (b) (d-e). The more intense color means a stronger interaction.

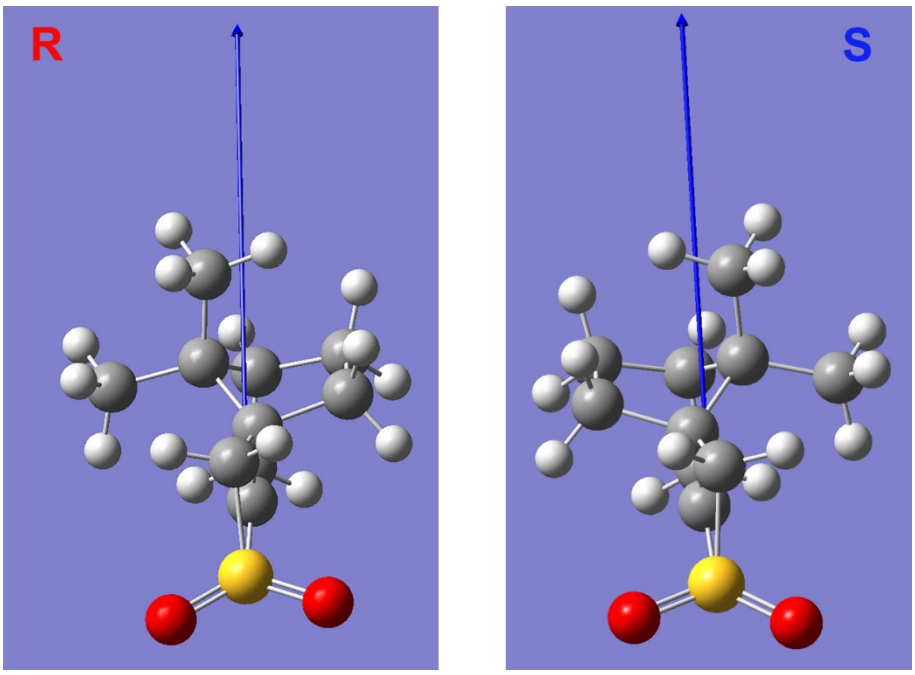

Fig. S3 Single molecule dipole moment of *R*-CSAI and *S*-CSAI calculated by Gauss 09.

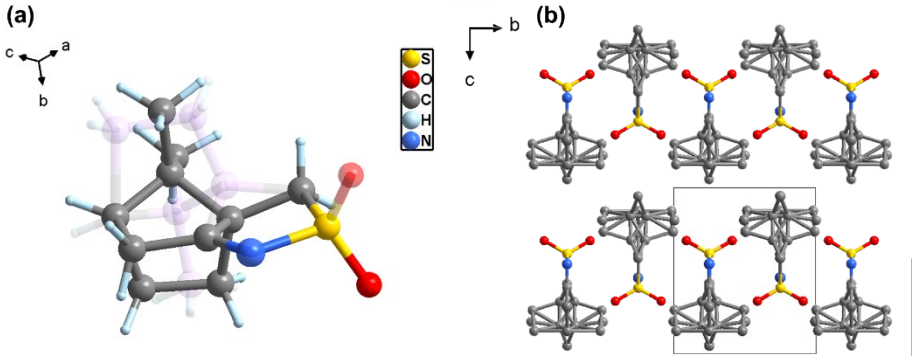

Fig. S4 Molecular structure (a) and crystal packing (b) of *Rac*-10-camphorsulfonylimine.

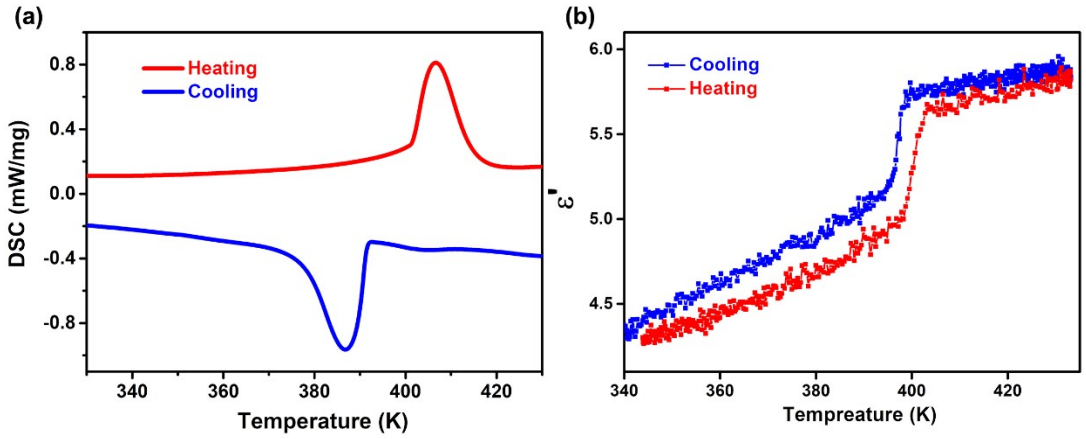

Fig. S5 The Phase transitions of *Rac*-10-camphorsulfonylimine. (a) DSC curves in a heating-cooling run. (b) Temperature-dependent permittivity ε′ at 1 MHz in the heating-cooling cycles.

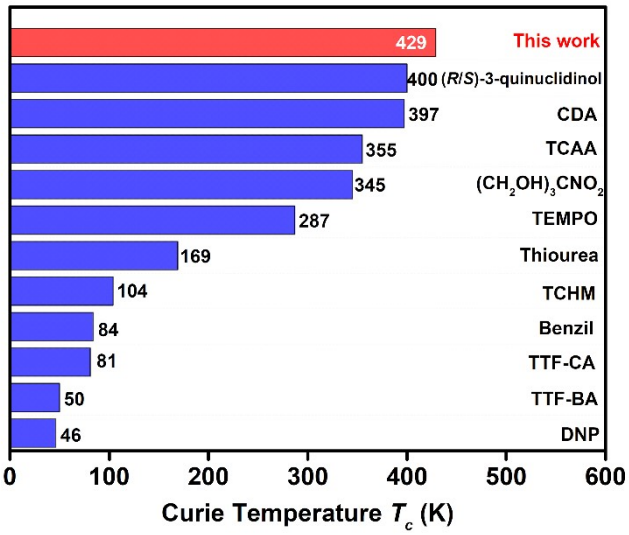

Fig. S6 Curie temperature T_c of R-CSAI and S-CSAI compared with some single-component molecular materials, including Thiourea[1], TEMPO[2], CDA[3], TCAA[4], Benzil[5], DNP[6], TCHM[7], TTF-CA[8], TTF-BA[9], *R*/*S*-3-quinuclidinol[10], $(CH_2OH)_3CNO_2$[11].

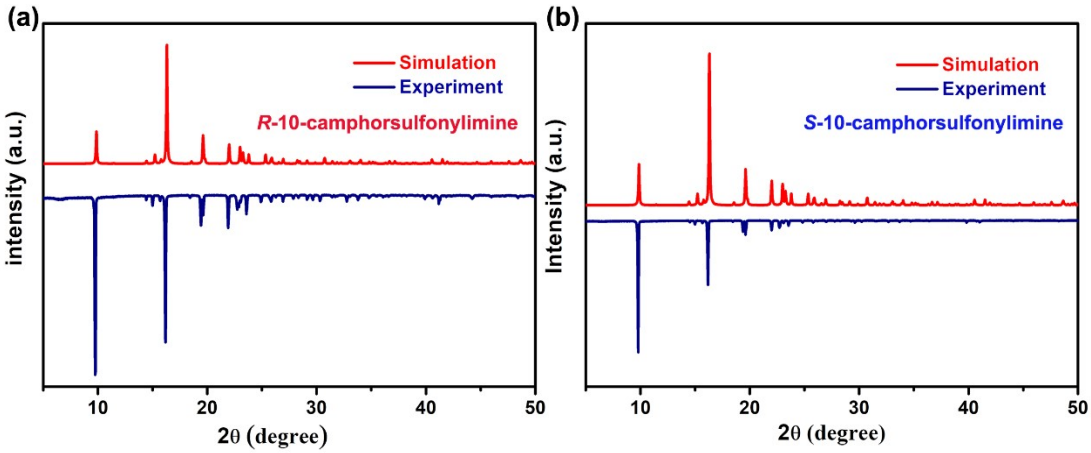

Fig. S7 Powder X-ray diffraction (PXRD) patterns of *R*-CSAI (a) and *S*-CSAI (b) matched well with the simulated from their crystal structure at room temperature.

(a)

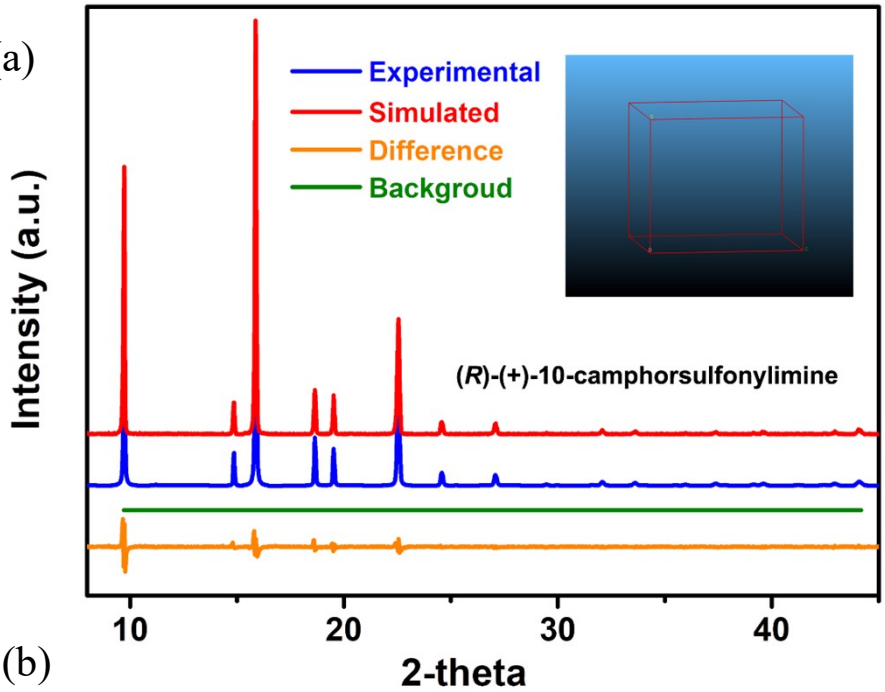

(b)

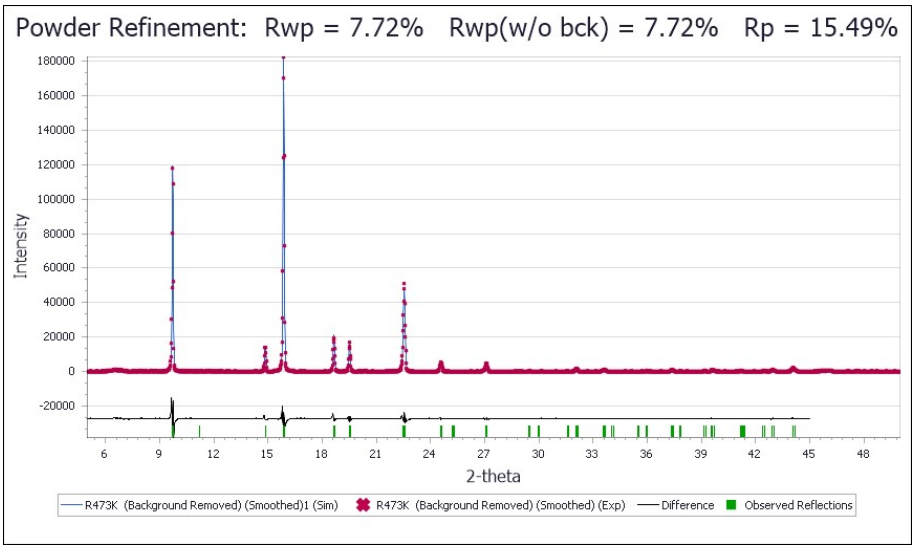

(c)

	F O M	Rwp	Space Gro	I T #	Option	System	a	b	c	alpha	beta	gamma	Volume
1	9.885207	7.824918	P4/N	85	Origin-1	Tetragona	7.915019	7.915019	9.114743	90	90	90	571.0161
2	9.885207	7.824918	P4/NMM	129	Origin-1	Tetragona	7.915019	7.915019	9.114743	90	90	90	571.0161
3	9.885207	7.824918	P4/NMM	129	Origin-2	Tetragona	7.915019	7.915019	9.114743	90	90	90	571.0161
4	9.885207	7.824918	P4/N	85	Origin-2	Tetragona	7.915019	7.915019	9.114743	90	90	90	571.0161
5	5.606479	7.824767	P4212	90	Origin-1	Tetragona	7.915019	7.915019	9.114743	90	90	90	571.0161
6	5.606479	7.824767	P-421M	113	Origin-1	Tetragona	7.915019	7.915019	9.114743	90	90	90	571.0161
7	0	7.852234	P-4	81	Origin-1	Tetragona	7.915019	7.915019	9.114743	90	90	90	571.0161
8	0	7.852234	P4/MMM	123	Origin-1	Tetragona	7.915019	7.915019	9.114743	90	90	90	571.0161
9	0	7.852234	P4MM	99	Origin-1	Tetragona	7.915019	7.915019	9.114743	90	90	90	571.0161
10	0	7.852234	P-4M2	115	Origin-1	Tetragona	7.915019	7.915019	9.114743	90	90	90	571.0161
11	0	7.852234	P-42M	111	Origin-1	Tetragona	7.915019	7.915019	9.114743	90	90	90	571.0161
12	0	7.852234	P422	89	Origin-1	Tetragona	7.915019	7.915019	9.114743	90	90	90	571.0161
13	0	7.852234	P4	75	Origin-1	Tetragona	7.915019	7.915019	9.114743	90	90	90	571.0161
14	0	7.852234	P4/M	83	Origin-1	Tetragona	7.915019	7.915019	9.114743	90	90	90	571.0161

Fig. S8 The final Rietveld refinement plot of *R*-CSAI structure at 473 K in HTP: experimental pattern (blue line), calculated pattern (red line), difference profile (yellow line) and background profile (green line). Through the Pawley refinements of the PXRD data, we obtained the tetragonal point group 422, among which the most possible space group is $P42_12$.

(a)

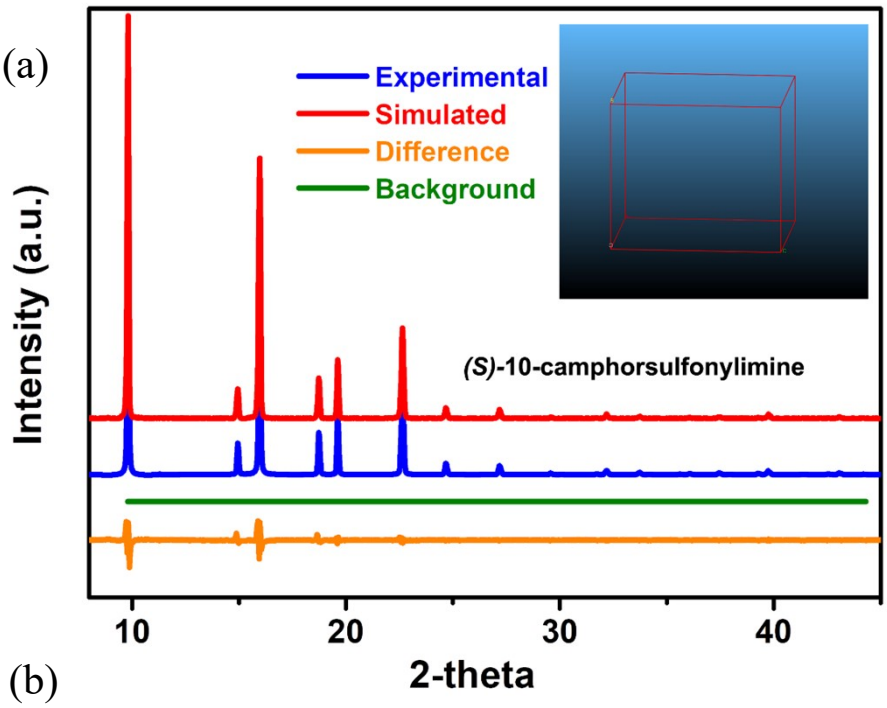

(b)

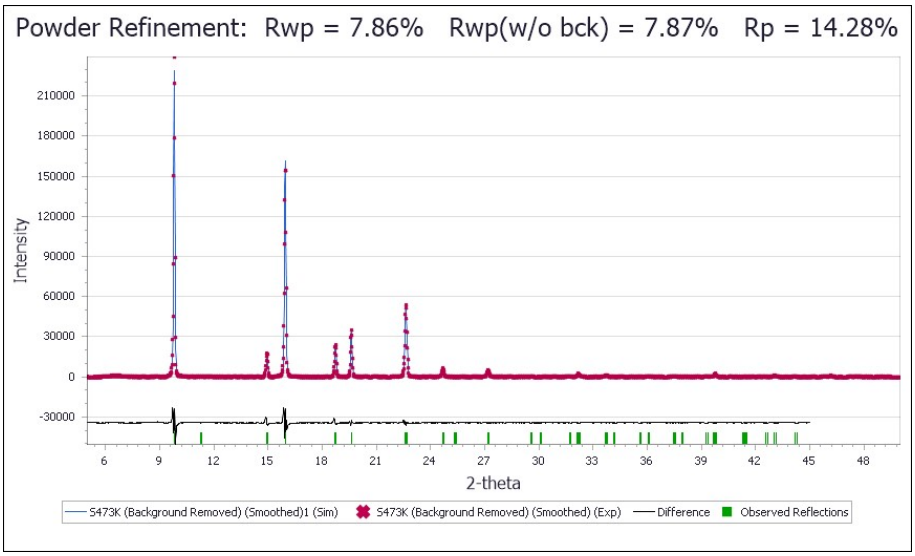

(c)

	F O M	Rwp	Space Gro	I T #	Option	System	a	b	c	alpha	beta	gamma	Volume
1	0	7.9731	P-4	81	Origin-1	Tetragona	7.884169	7.884169	9.07676	90	90	90	564.2125
2	0	7.9731	P-4M2	115	Origin-1	Tetragona	7.884169	7.884169	9.07676	90	90	90	564.2125
3	0	7.9731	P4	75	Origin-1	Tetragona	7.884169	7.884169	9.07676	90	90	90	564.2125
4	0	7.9731	P4/M	83	Origin-1	Tetragona	7.884169	7.884169	9.07676	90	90	90	564.2125
5	0	7.9731	P-42M	111	Origin-1	Tetragona	7.884169	7.884169	9.07676	90	90	90	564.2125
6	0	7.9731	P422	89	Origin-1	Tetragona	7.884169	7.884169	9.07676	90	90	90	564.2125
7	0	7.9731	P4/MMM	123	Origin-1	Tetragona	7.884169	7.884169	9.07676	90	90	90	564.2125
8	0	7.9731	P4MM	99	Origin-1	Tetragona	7.884169	7.884169	9.07676	90	90	90	564.2125
9	-10.3843	7.946417	P4/N	85	Origin-1	Tetragona	7.884169	7.884169	9.07676	90	90	90	564.2125
10	-10.3843	7.946417	P4/NMM	129	Origin-1	Tetragona	7.884169	7.884169	9.07676	90	90	90	564.2125
11	-10.3843	7.946417	P4/N	85	Origin-2	Tetragona	7.884169	7.884169	9.07676	90	90	90	564.2125
12	-10.3843	7.946417	P4/NMM	129	Origin-2	Tetragona	7.884169	7.884169	9.07676	90	90	90	564.2125
13	-14.7896	7.946393	P4212	90	Origin-1	Tetragona	7.884169	7.884169	9.07676	90	90	90	564.2125
14	-14.7896	7.946393	P-421M	113	Origin-1	Tetragona	7.884169	7.884169	9.07676	90	90	90	564.2125
15	-62.1271	13.26154	P4/NBM	125	Origin-2	Tetragona	7.884169	7.884169	9.07676	90	90	90	564.2125

Fig. S9 The final Rietveld refinement plot of *S*-CSAI structure at 473 K in HTP: experimental pattern (blue line), calculated pattern (red line), difference profile (yellow line) and background profile (green line). Through the Pawley refinements of the PXRD data, we obtained the tetragonal point group 422, among which the most possible space group is *P*422 or $P42_12$.

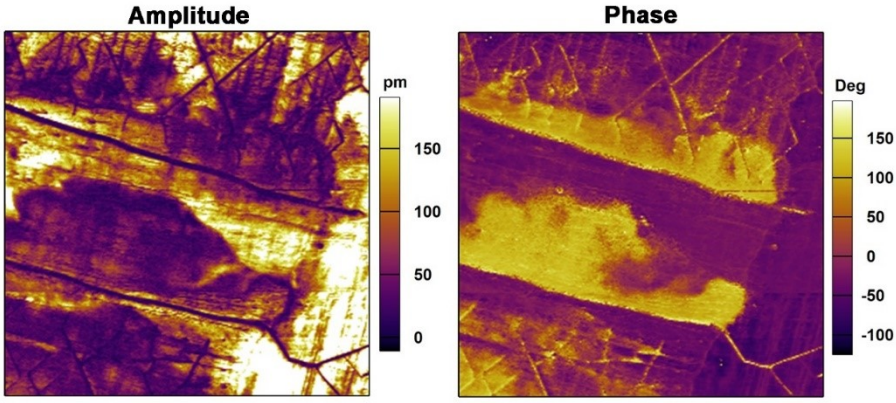

Fig. S10 Vertical PFM imaging for the same region shown in Fig. 6a-c.

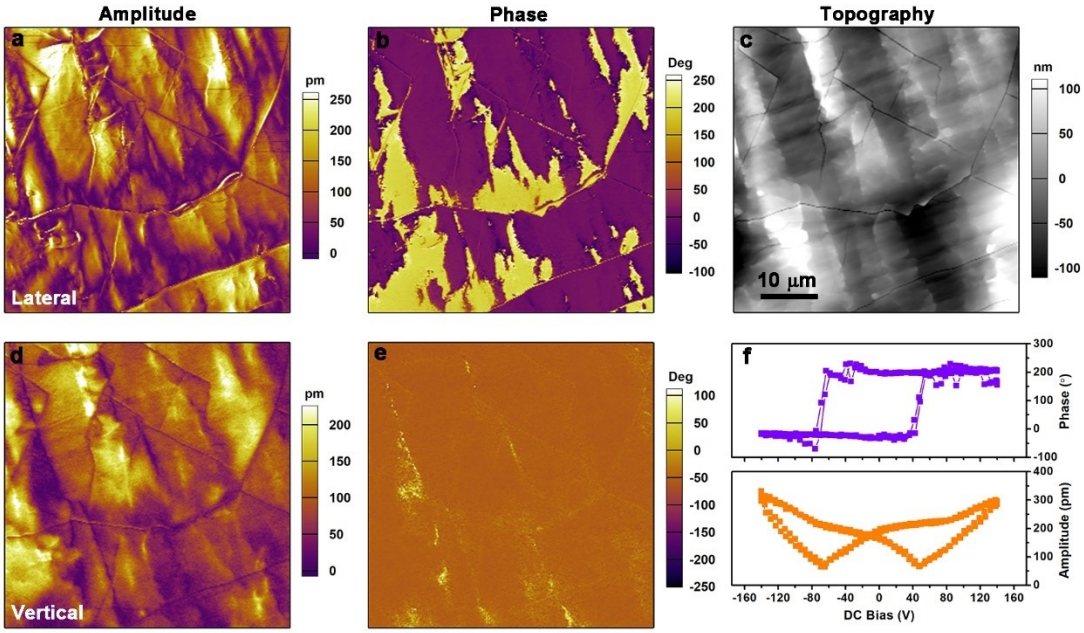

Fig. S11 The diagrams of lateral amplitude (a), phase (b), topology (c) vertical amplitude (d), phase (e) and switching spectroscopy (f) of *R*-CSAI thin film taken by PFM.

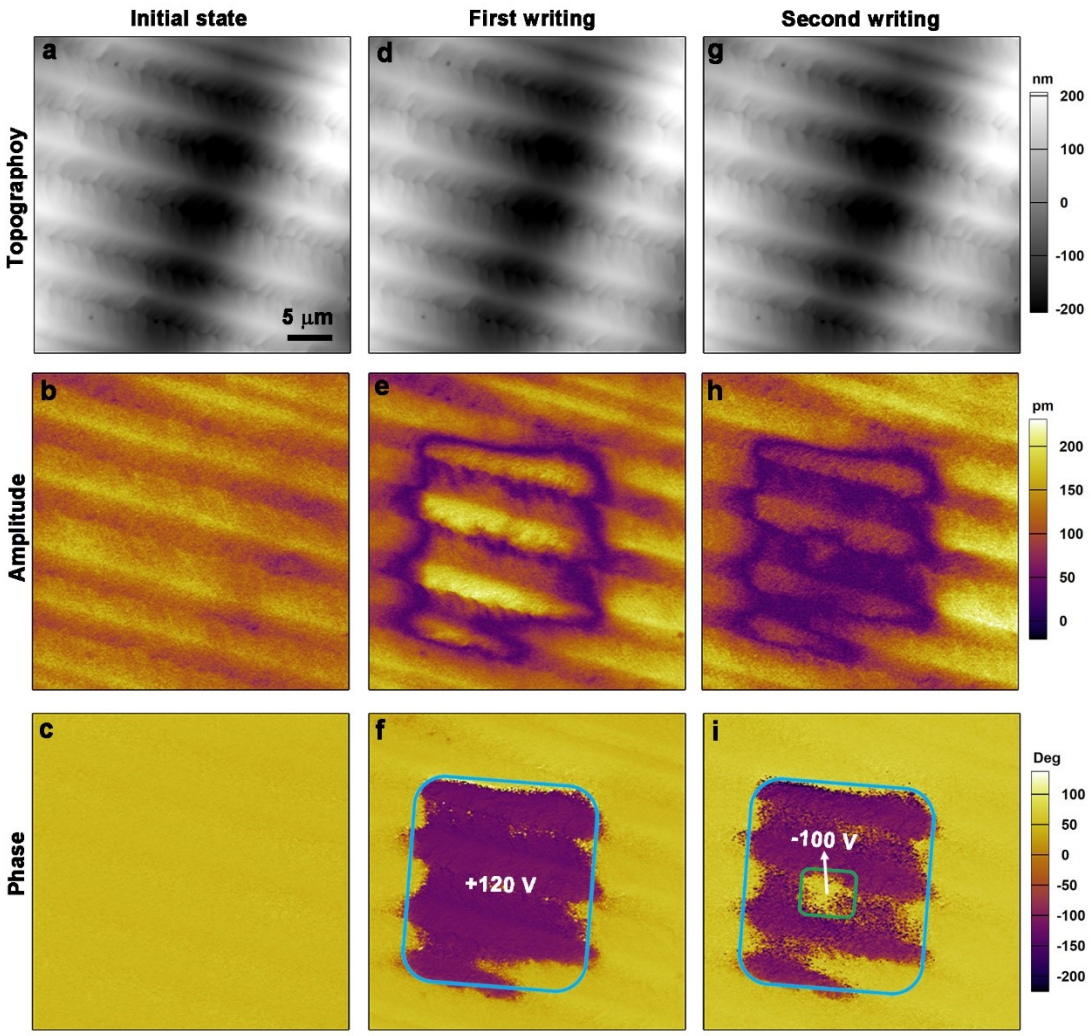

Fig. S12 Domain switching measurements for the *R*-CSAI thin film. The panels in each row are arranged as the sequence: the topographic images (up), the vertical PFM amplitude images (middle) and the phase images (bottom). (a–c) PFM images of the as-prepared thin-film surface. (d–f) PFM images after the first polarization writing with positive tip-bias of +120 V. (g–i) PFM images after the second polarization writing in a smaller area with tip-bias of -100 V.

Table S1. Crystal data for *R*-CSAI and *S*-CSAI at 173 K and 298 K, *Rac*-10-CSAI at 100 K.

Temperature	173 K	298 K	173 K	298 K	100 K
Compound	*R*-CSAI	*R*-CSAI	*S*-CSAI	*S*-CSAI	*Rac*-CSAI
Formula	$C_{10}H_{15}NO_2S$	$C_{10}H_{15}NO_2S$	$C_{10}H_{15}NO_2S$	$C_{10}H_{15}NO_2S$	$C_{10}H_{15}NO_2S$
Weight	213.29	213.29	213.29	213.29	213.29
Crystal system	Monoclinic	Monoclinic	Monoclinic	Monoclinic	Monoclinic
Space group	$P2_1$	$P2_1$	$P2_1$	$P2_1$	$P2_1$/m
a / Å	7.74800 (10)	7.7200(2)	7.7527 (3)	7.7253(5)	7.6990(1)
b / Å	7.63120 (10)	7.7534(2)	7.6368 (3)	7.7557(4)	7.6119(1)
c / Å	8.99860 (10)	9.0532(2)	8.9989 (4)	9.0549(5)	8.9599(1)
α / °	90	90	90	90	90
β / °	95.1100	94.725	95.097	94.727	94.873(1)
γ / °	90	90	90	90	90
V / Å^3	529.941 (11)	540.05	530.68 (4)	540.68	523.188(11)
Z	2	2	2	2	2
R_1	0.0295	0.0519	0.0268	0.0355	0.0348
wR_2	0.0810	0.1384	0.0734	0.0962	0.0871
GOF	1.029	1.074	1.059	1.054	1.116
Flack	0.020(16)	0.01(2)	-0.06(4)	0.02(5)	

Table S2. List of z_0 measured values on different ferroelectric samples.

Ferroelectrics	ρ 10^3 kg·m^{-3}	c 10^3 m·s^{-1}	z_0 10^6 kg·s^{-1}·m^{-2}
TGS crystal	1.69	5.76	9.74
$BaTiO_3$ crystal	5.30	3.97	21.05
$LiNbO_3$ crystal	4.34	10.06	43.64
Diisopropylammonium bromide crystal	1.34	3.27	4.39
Rochelle salt crystal	1.79	4.21	7.54
PZT 52:48 ceramics	7.50	3.39	25.39
TMCM-$MnCl_3$ polycrystal	1.83	3.48	6.38
TMCM-$CdCl_3$ polycrystal	2.15	3.42	7.35
PVDF standard	1.78	2.39	4.25
PVDF thermal pressing	1.63	2.26	3.69
Tris(hydroxymethyl)nitromethane polycrystal	1.38	6.01	8.20
Phenylammonium bromide polycrystal	1.59	3.21	5.11
(*R* and *S*)-3-hydroxyquinoline	1.17	2.90	3.39
(*R* and *S*)-CASI (This work)	1.17	2.09	**2.45**

REFREENCE

1. G. J. Goldsmith, J. G. White, Ferroelectric behavior of thiourea. *J. Chem. Phys.* 1959, **31**, 1175.
2. D. Bordeaux, J. Bornarel, A. Capiomont, J. Lajzerowicz-Bonneteau, J. Lajzerowicz, J. F. Legrand, *Phys. Rev. Lett.* 1973, **31**, 314.
3. J. Kroupa, P. Vaněk, R. Krupková, Z. Zikmund, *Ferroelectrics* 1997, **202**, 229.
4. M. Hiraoka, T. Hasegawa, To. Yamada, Y. Takahashi, S. Horiuchi, Y. Tokura, *Adv. Mater.* 2007, **19**, 3248.
5. Y. Akishige, Y. Kamishima, *J. Phys. Soc. Jpn.* 2001, **70**, 3124.
6. H. Schultes, P. Strohriegl, E. Dormann, *Ferroelectrics* 1986, **70**, 161.
7. P. Szklarz, G. Bator, *J. Phys. Chem. Solids* 2005, **66**, 121.
8. H. Okamoto, T. Mitani, Y. Tokura, S. Koshihara, T. Komatsu, Y. Iwasa, T. Koda, G. Saito *Phys. Rev. B* 1991, **43**, 8224.
9. Y. Tokura, S. Koshihara, Y. Iwasa, H. Okamoto, T. Komatsu, T. Koda, N. Iwasawa, G. Saito, *Phys. Rev. Lett.* 1989, **63**, 2405.
10. P. F. Li, W. Q. Liao, Y. Y. Tang, W. C. Qiao, D. W. Zhao, Y. Ai, Y. F. Yao, R. G. Xiong, *P. Natl. Acad. Sci. USA* **2019**, *116*, 5878.
11. Y. Ai, Y. L. Zeng, W. H. He, X. Q. Huang, Y. Y. Tang, *J. Am. Chem. Soc.* **2020**, *142*, 13989